

## Terephthalamide Derivatives as Mimetics of Helical Peptides: Disruption of the Bcl-x<sub>L</sub>/Bak Interaction

Hang Yin,<sup>†</sup> Gui-in Lee,<sup>†</sup> Kristine A. Sedey,<sup>‡</sup> Johanna M. Rodriguez,<sup>†</sup>  
Hong-Gang Wang,<sup>‡</sup> Said M. Sebt,<sup>‡</sup> and Andrew D. Hamilton<sup>\*,†</sup>

Contribution from the Department of Chemistry, Yale University, P.O. Box 208107,  
New Haven, Connecticut 06520-8107, and Drug Discovery Program,  
H. Lee Moffitt Cancer Center and Research Institute, Departments of Oncology and  
Biochemistry and Molecular Biology, University of South Florida, Tampa, Florida 33612

Received September 3, 2004; E-mail: andrew.hamilton@yale.edu

**Abstract:** A series of Bcl-x<sub>L</sub>/Bak antagonists, based on a terephthalamide scaffold, was designed to mimic the  $\alpha$ -helical region of the Bak peptide. These molecules showed favorable in vitro activities in disrupting the Bcl-x<sub>L</sub>/Bak BH3 domain complex (terephthalamides **9** and **26**,  $K_i = 0.78 \pm 0.07$  and  $1.85 \pm 0.32 \mu\text{M}$ , respectively). Extensive structure–affinity studies demonstrated a correlation between the ability of terephthalamide derivatives to disrupt Bcl-x<sub>L</sub>/Bak complex formation and the size of variable side chains on these molecules. Treatment of human HEK293 cells with the terephthalamide derivative **26** resulted in disruption of the Bcl-x<sub>L</sub>/Bax interaction in whole cells with an IC<sub>50</sub> of 35.0  $\mu\text{M}$ . Computational docking simulations and NMR experiments suggested that the binding cleft for the BH3 domain of the Bak peptide on the surface of Bcl-x<sub>L</sub> is the target area for these synthetic inhibitors.

### Introduction

Proteins in the B-cell lymphoma-2 (Bcl-2) family play a critical role in determining whether a cell survives or dies through a programmed cell death known as apoptosis.<sup>1</sup> The Bcl-2 protein family, comprised of both pro-apoptotic and anti-apoptotic members, acts as a checkpoint downstream of the tumor suppressor protein p53,<sup>2</sup> and upstream of mitochondrial membrane rupture and caspase cysteine proteases, which transduce the apoptotic signal.<sup>1</sup> Previous studies showed that oncogenic mutations induced apoptosis defects through a Bcl-2-dependent pathway.<sup>3</sup> Overexpression of the anti-apoptotic proteins, such as Bcl-2 and Bcl-x<sub>L</sub>, can inhibit the potency of many currently available anticancer drugs by blocking the apoptotic pathway.<sup>4</sup> All of the pro-apoptotic subfamily proteins possess the minimal death domain BH3. These molecules (Bak, Bax, Bad, Bid) are able to induce apoptosis through heterodimerization with the anti-apoptotic Bcl-2 family members.<sup>5</sup> Several low-molecular-weight inhibitors of Bcl-2 (Bcl-x<sub>L</sub>) have been identified by screening diverse chemical libraries.<sup>6,7</sup> The rational design of agents that directly mimic the death-promoting region, the BH3 domain of the pro-apoptotic subfamily of Bcl-2 proteins, is an important alternative to screening as it allows structure-based optimization of initial hits.<sup>8</sup>

The development of small-molecule modulators of protein–protein interactions is regarded as a challenging goal since the large interfaces involved, typically around 1600 Å<sup>2</sup> of buried area (around 170 atoms), pose a serious hurdle for any small molecule to be competitive.<sup>9</sup> The binding regions of protein partners are often discontinuous and thus cannot be mimicked by simple synthetic peptides with linear or extended conformations. Conventional methods for identifying inhibitors of protein–protein interactions require much input in the preparation and screening of a chemical library in order to discover lead compounds. An alternative approach is to design synthetic recognition scaffolds that reproduce features of the protein secondary structure at the interface. We have previously reported functionalized terphenyls as mimetics of  $\alpha$ -helices.<sup>10,11</sup> However, the challenging syntheses and physical properties of terphenyls prompted us to search for simpler scaffolds that could similarly mimic the side chain presentation on an  $\alpha$ -helix.<sup>12</sup> We have recently reported a group of Bcl-x<sub>L</sub> inhibitors based on a terephthalamide scaffold, designed to mimic the  $\alpha$ -helical region

<sup>†</sup> Yale University.

<sup>‡</sup> University of South Florida.

- (1) Adams, J. M.; Cory, S. *Science* **1998**, *281*, 1322–1326. Reed, J. C.; *Nature* **1997**, *387*, 773–776.
- (2) Lane, D. P. *Nature* **1992**, *358*, 15–16.
- (3) Graeber, T. G.; Osmanian, C.; Jacks, T.; Housman, D. E.; Koch, C. J.; Lowe, S. W.; Giaccia, A. J. *Nature* **1996**, *379*, 88–91. Fearon, E. R.; Vogelstein, B. *Cell* **1990**, *61*, 759–767.
- (4) Strasser, A.; Huang, D. C. S.; Vaux, D. L. *Biochim. Biophys. Acta–Rev. Cancer* **1997**, *1333*, F151–F178.
- (5) Chao, D. T.; Korsmeyer, S. J. *Annu. Rev. Immunol.* **1998**, *16*, 395–419.

- (6) Tzung, S. P.; Kim, K. M.; Basanez, G.; Giedt, C. D.; Simon, J.; Zimmerberg, J.; Zhang, K. Y. J.; Hockenbery, D. M. *Nat. Cell Biol.* **2001**, *3*, 183–191. Enyedy, I. J.; Ling, Y.; Nacro, K.; Tomita, Y.; Wu, X. H.; Cao, Y. Y.; Guo, R. B.; Li, B. H.; Zhu, X. F.; Huang, Y.; Long, Y. Q.; Roller, P. P.; Yang, D. J.; Wang, S. M. *J. Med. Chem.* **2001**, *44*, 4313–4324. Wang, J. L.; Liu, D. X.; Zhang, Z. J.; Shan, S. M.; Han, X. B.; Srinivasula, S. M.; Croce, C. M.; Alnemri, E. S.; Huang, Z. W. *Proc. Natl. Acad. Sci. U.S.A.* **2000**, *97*, 7124–7129. Lugovskoy, A. A.; Degterev, A. I.; Fahmy, A. F.; Zhou, P.; Gross, J. D.; Yuan, J. Y.; Wagner, G. *J. Am. Chem. Soc.* **2002**, *124*, 1234–1240.
- (7) Degterev, A.; Lugovskoy, A.; Cardone, M.; Mulley, B.; Wagner, G.; Mitchison, T.; Yuan, J. Y. *Nat. Cell Biol.* **2001**, *3*, 173–182.
- (8) Adams, J. M.; Cory, S. *Trends Biochem. Sci.* **2001**, *26*, 61–66.
- (9) Stites, W. E. *Chem. Rev.* **1997**, *97*, 1233–1250.
- (10) Orner, B. P.; Ernst, J. T.; Hamilton, A. D. *J. Am. Chem. Soc.* **2001**, *123*, 5382–5383.
- (11) Kutzi, O.; Park, H. S.; Ernst, J. T.; Orner, B. P.; Yin, H.; Hamilton, A. D. *J. Am. Chem. Soc.* **2002**, *124*, 11838–11839.

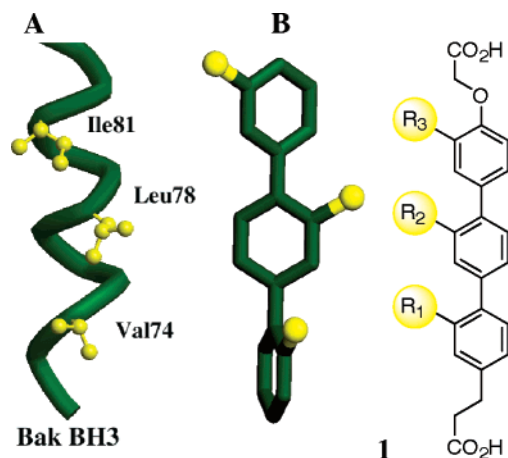


**Figure 1.** (A) NMR structure of the Bak BH3 domain complex.<sup>14</sup> The side chains of Val74, Leu78, and Ile81 residues (shown in yellow) play critical roles in the Bcl-x<sub>L</sub>/Bak complex formation. (B) Generic structure of terphenyl  $\alpha$ -helical mimetics. An energy-minimized structure shows that the spatial arrangement of 3,2',2''-side chains on the terphenyl scaffold has a good agreement with those at the *i*, *i*+4, and *i*+7 positions on an  $\alpha$ -helix.<sup>15</sup>

of the Bak peptide.<sup>13</sup> Using a fluorescence polarization assay, we have observed high in vitro inhibition potencies in disrupting the Bcl-x<sub>L</sub>/Bak BH3 domain complex and a significant improvement in water solubility relative to the terphenyl derivatives. In this report, we present an expanded structure–affinity study that demonstrates a correlation between the potency of the Bcl-x<sub>L</sub>/Bak disruption and the size of side chains on these molecules. Computational docking simulations and NMR experiments are used to confirm the binding mode of the terephthalamide inhibitors and suggest that the binding cleft for the Bak BH3 domain on the surface of Bcl-x<sub>L</sub> is the target area. Treatment of human HEK293 cells with one of the terephthalamide derivatives resulted in inhibition of the association of Bcl-x<sub>L</sub> with Bax in whole cells.

## Results and Discussion

**Inhibitor Design.** The NMR-derived structure of the Bcl-x<sub>L</sub>/Bak BH3 domain complex indicates that the Bak BH3 peptide is an amphipathic  $\alpha$ -helix that interacts with Bcl-x<sub>L</sub> by projecting hydrophobic side chains (Val74, Leu78, Ile81, and Ile85) on one face of the  $\alpha$ -helix into a hydrophobic cleft of Bcl-x<sub>L</sub> (Figure 1A).<sup>14</sup> We have reported terphenyl derivatives (**1**) as structural mimetics of the Bak BH3 helical peptide as they adopt a staggered conformation and project appropriately positioned substituents in a manner similar to an  $\alpha$ -helix (Figure 1B).<sup>11</sup>

The design of a next generation of helical mimetics should maintain the similarity between the arrangement of the *i*, *i*+4, *i*+7 side chains of an  $\alpha$ -helix and the substituents on 3,2',2''-positions on terphenyl **1**, while minimizing the structural complexity and increasing the rigidity and solubility of the inhibitors. This strategy of simplifying a proven *proteomimetic* was accomplished by using terephthalamide **2** as the scaffold. The flanking phenyl rings in **1** were replaced by two functionalized carboxamide groups, which retain the planar geometry

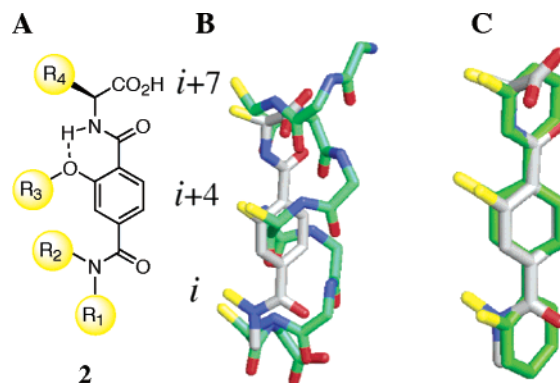


**Figure 2.** (A) Generic structure of terephthalamide helical mimetics. (B) The superimposition of **2** on the *i*, *i*+4, *i*+7 positions of an  $\alpha$ -helix (RMSD = 1.03 Å). (C) The superimposition of terphenyl **1** and terephthalamide **2** (RMSD = 0.34 Å). The functionalized side chains are highlighted.

of the phenyl rings, due to the restricted rotation of the amide bonds. Another conformational constraint in the molecule was imposed by an intramolecular hydrogen bond between the amide –NH and the alkoxy oxygen atom, to influence the position of the amino acid side chain R<sub>4</sub> (Figure 2A). The modularity of the inhibitor synthesis is strengthened since terphenyl **1** requires difficult C–C bond formations to attach the side chains to the scaffold and to assemble functionalized phenyl building blocks.<sup>10,11</sup> Terephthalamide derivatives, on the other hand, were synthesized using O-alkylation and amide formations, accelerating the process of preparing these compounds.

The newly introduced carboxamide groups also increase the polarity of the inhibitors. One limitation of the terphenyl derivatives is their high hydrophobicity. Calculations using the QikProp program predicted that terephthalamide **26** has a logP (partition coefficient for *n*-octanol/water) of 4.42, compared to 9.25 for terphenyl **1** (R<sub>1</sub> = R<sub>3</sub> = *i*Bu, R<sub>2</sub> = 1-naphthylmethylene), suggesting that terephthalamides should have more favorable properties within an acceptable log *P* range (–2 to 6).<sup>16,17</sup> Structure-based solubility prediction showed that **26** has a log *S* (aqueous solubility) of –5.35, compared to –10.76 for **1**, suggesting that terephthalamide derivatives should have improved solubility in aqueous solution.<sup>18</sup>

The preferred conformation of terephthalamide derivatives in solution was investigated using energy minimization with the MM2 force field (Macromodel 7.0). Parts B and C of Figure 2 show, respectively, superimpositions of the energy-minimized conformation of **2** on the *i*, *i*+4, *i*+7 side chains of an  $\alpha$ -helix (with a root-mean-square deviation (RMSD) value of 1.03 Å) and on a terphenyl scaffold (RMSD = 0.34 Å), suggesting good stereochemical similarity between the two pairs.<sup>19</sup>

Two strategies were used to orient the interacting N-alkyl group R<sub>2</sub> of the lower tertiary amide into the desired *Z*-conformation. The first was to avoid the problem by using identical substituents (R<sub>1</sub> = R<sub>2</sub>) on the tertiary amide nitrogen.

- (12) Lipinski, C. A.; Lombardo, F.; Dominy, B. W.; Feeney, P. J. *Adv. Drug Deliver. Rev.* **1997**, *23*, 3–25.
- (13) Yin, H.; Hamilton, A. D. *Bioorg. Med. Chem. Lett.* **2004**, *14*, 1375–1379.
- (14) Sattler, M.; Liang, H.; Nettesheim, D.; Meadows, R. P.; Harlan, J. E.; Eberstadt, M.; Yoon, H. S.; Shuker, S. B.; Chang, B. S.; Minn, A. J.; Thompson, C. B.; Fesik, S. W. *Science* **1997**, *275*, 983–986.

- (15) Energy minimization was carried out using MM2 force field within Macromodel V7.0.
- (16) Jorgensen, W. L.; Duffy, E. M. *Adv. Drug Deliver. Rev.* **2002**, *54*, 355–366; Jorgensen, W. L.; Duffy, E. M. *Bioorg. Med. Chem. Lett.* **2000**, *10*, 1155–1158.
- (17) Jorgensen, W. L. *Science* **2004**, *303*, 1813–1818.
- (18) The log *P* and log *S* calculations were carried out using QikProp V2.1 (Shrodinger Inc., New York, 2003). Huuskonen et al. have shown that 85% of drugs have log *S* values between –1 and –5, and virtually none has a value below –6 (*J. Chem. Inf. Comput. Sci.* **1998**, *38*, 450–456).
- (19) Ernst, J. T.; Becerril, J.; Park, H. S.; Yin, H.; Hamilton, A. D. *Angew. Chem.-Int. Edit.* **2003**, *42*, 535–550.

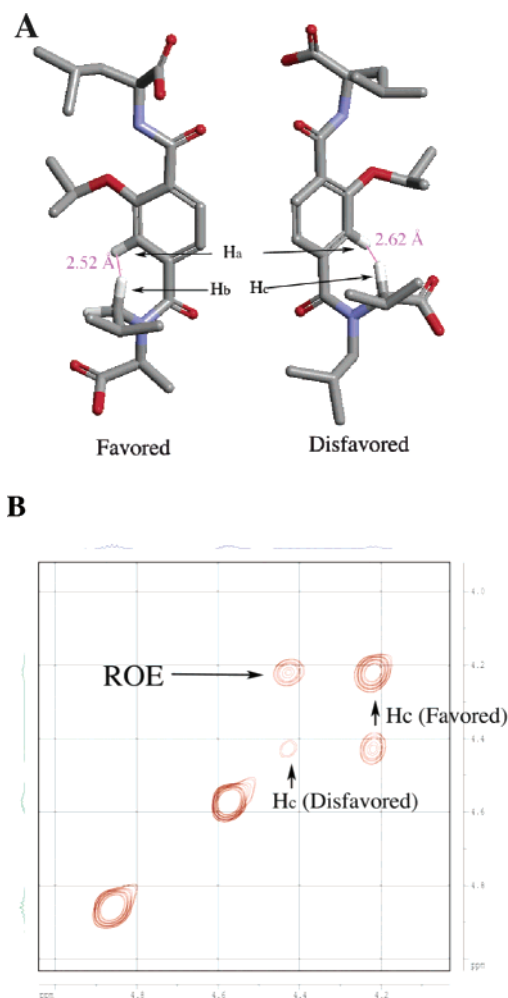
In a second series of derivatives, such as **22**, steric differentiation of the substituents favored the placement of the less bulky group  $R_3$  in the *Z*-position. The consequence of these constraints is that in low-energy, accessible conformations of **22**, the three substituents project from one face of the terephthalamide scaffold in a manner analogous to the terphenyl helix mimetics (e.g. Figure 2A).

**Conformational Studies.** The intramolecular hydrogen bond between the amide  $-NH$  and the alkoxy oxygen atom of **9** ensures that the 2-isopropoxy group and the upper isobutyl side chain are positioned on the same side of the terephthalamide. This hydrogen bond was confirmed by proton NMR experiments, which showed very little change in the amide  $-NH$  resonance ( $\delta = 8.54$  ppm) on heating ( $\Delta\delta = 1.54$  ppb/K) or changing concentration. As a comparison, 2-isopropylamino-terephthalamide **17** showed both concentration (7.36 ppm, 0.5 M in  $CDCl_3$ ; 6.58 ppm, 0.05 M in  $CDCl_3$ ; 6.46 ppm, 0.005 M in  $CDCl_3$ , 298 K) and temperature ( $\Delta\delta = 5.5$  ppb/K) dependence of the aniline proton, suggesting inter- rather than intramolecular hydrogen bonding.

The conformation of the lower tertiary amide in **22** in solution was probed by computational simulations and  $^1H$  NMR spectroscopy. MM2 energy minimization using MacroModel suggested that the *Z*-conformation is favored by 8.01 kJ/mol in water solution (Figure 3A), and indeed NMR integration indicated that 72% of **22** adopted the *Z*-conformation in chloroform solution. Computer simulation showed that  $H_b$  and  $H_c$  have similar distances to the ortho-proton  $H_a$  in the *Z*- and *E*-conformations (2.52 and 2.62 Å, respectively). However, only the nuclear Overhauser effect (NOE) cross-peaks between  $H_b$  and the ortho-aryl proton  $H_a$  were detected, while no significant NOE effect could be seen between  $H_c$  and  $H_a$ , suggesting the *Z*- is the major conformation in solution. Rotational Overhauser effect spectroscopy (ROESY) confirmed the presence of both *Z*- and *E*-conformations. Correlations corresponding to the chemical exchange of  $H_b$  and  $H_c$  were observed in the ROESY experiment (Figure 3B), which indicated that both conformations of **22** exist in DMSO solution at 298 K. Furthermore, the signals of both  $H_a$  and  $H_b$ , which are split at room temperature, coalesced at 353 K. These combined experimental results suggest that both *Z*- and *E*-amide conformations are present with the *Z*-conformation being favored.

**In Vitro Fluorescence Polarization Assay.** The binding affinity of the terephthalamide molecules for Bcl- $x_L$  was assessed by a previously reported fluorescence polarization assay using a fluorescently labeled 16-mer Bak-peptide (FI-GQVGRQLAIGDDINR-CONH $_2$ ).<sup>14</sup> Displacement of this probe through competitive binding of the terephthalamide into the hydrophobic cleft of Bcl- $x_L$  leads to a decrease in its fluorescence polarization. Computational regression analysis was conducted to determine the  $IC_{50}$  values, which in turn can be related to the known affinity of the 16-mer Bak peptide ( $K_d = 120$  nM) to acquire the inhibitory constant ( $K_i$ ) of the inhibitors.<sup>11,20</sup> To test the validity of this assay, we used a nonlabeled Bak-peptide as the competitive inhibitor to bind Bcl- $x_L$ , giving a  $K_i$  of 122 nM, which closely corresponds to the  $K_d$  value obtained from the saturation titration experiment.

A series of terephthalamides with varied side chains were prepared. All the assays were carried out with 0.01–1000  $\mu M$

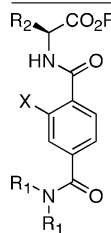
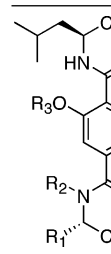


**Figure 3.** (A) Energy minimized *Z*- and *E*-isomers of **22**. (B) ROESY  $^1H$ – $^1H$  NMR experiments showed cross-peaks corresponding to the chemical exchange of  $H_c$ .

terephthalamide solution in 10 mM PBS buffer (pH = 7.4, 298 K) with less than 0.1% DMSO, a testament to the good solubility of terephthalamides in water. Table 1 shows that terephthalamide **9** has good affinity for Bcl- $x_L$  with a  $K_i$  value of  $0.78 \pm 0.07$   $\mu M$ . By screening compounds with a range of side chains on the upper carboxamide, we found that the isobutyl group as the upper substituent provided the best inhibition results (**9**, **10**, **29**, **34**). The newly introduced stereogenic center in the terephthalamide did not affect the affinity, as seen by comparing **26** and **27**. The optimal alkoxy group in the 2-position of terephthalamide was found to be isopropoxy (**9**, **10**, **34**, **37**), which closely mimics the size of Leu78 of the Bak peptide; both larger (**29**, **31**) and smaller (**26**, **27**) substituents gave decreased affinities. The *N,N*-alkyl positions on the lower carboxamide were shown to favor the medium to small substituents since *N,N*-dimethyl (**34**), -diethyl (**37**), and -diisopropyl (**9**, **10**) terephthalamide analogues have low micromolar  $K_i$  values while most of the affinity was lost when the alkyl substituents were replaced by phenyl groups (**42**–**45**). Comparison of the terephthalamide derivatives with the free amino acid in the upper carboxamide moiety and their methyl esters suggested that the ester group did not significantly affect the binding (**9**, **10**, and **26**–**28**). However, for less hydrophilic compounds, such as **31** and **32**, only the free acid derivatives are soluble in aqueous solution. The 2-isopropylamino terephthalamide **17** showed



**Table 1.** Results of the Fluorescence Polarization Competition Assay of Terephthalamide Derivatives as the Antagonists of Bcl-x<sub>L</sub>/Bak Complex

	R <sub>1</sub>	X	R <sub>2</sub>	R <sub>3</sub>	entry	K <sub>i</sub> ± SD (μM) <sup>a</sup>
	-iPr	-OiPr	-iBu	-Me	<b>9</b>	0.78 ± 0.07
			-iBu	-H	<b>10</b>	0.84 ± 0.17
			-Me	-Me	<b>23</b>	11.0 ± 1.9
			-iPr	-Me	<b>24</b>	5.85 ± 2.07
			-Bn	-Me	<b>25</b>	10.9 ± 5.17
		-OMe	(S)-iBu	-Me	<b>26</b>	1.85 ± 0.32
			(R)-iBu	-Me	<b>27</b>	1.79 ± 0.39
			(S)-iBu	-H	<b>28</b>	2.31 ± 0.33
		-OPh	-iBu	-H	<b>29</b>	1.01 ± 0.05
			-iBu	-Me	<b>30</b>	not soluble
		-O(2-naphthyl)	-iBu	-H	<b>31</b>	7.63 ± 1.02
		-O( <i>p</i> -nitrophenyl)	-iBu	-Me	<b>32</b>	13.2 ± 8.8
		-NH( <i>i</i> Pr)	-iBu	-H	<b>17</b>	3.31 ± 0.35
	-Me	-OiPr	-Me	-Me	<b>33</b>	8.34 ± 1.61
			-iBu	-Me	<b>34</b>	3.14 ± 0.31
			-Bn	-H	<b>35</b>	8.92 ± 3.59
		H	-H	-Me	<b>36</b>	no affinity
	-Et	-OiPr	-Me	-Me	<b>37</b>	2.44 ± 0.95
			-iBu	-Me	<b>38</b>	11.4 ± 5.1
	-iBu	-OiPr	-Me	-Me	<b>39</b>	8.76 ± 2.78
			-iBu	-Me	<b>40</b>	8.36 ± 3.80
			-iPr	-Me	<b>41</b>	138 ± 50
	-Ph	-OiPr	-Me	-H	<b>42</b>	260 ± 58
			-iBu	-H	<b>43</b>	780 ± 174
			-iBu	-Me	<b>44</b>	no affinity
			-Bn	-H	<b>45</b>	no affinity
	R <sub>1</sub>	R <sub>2</sub>	R <sub>3</sub>	R <sub>4</sub>	Entry	K <sub>i</sub> ± SD (μM)
	-Me	-iBu	-iPr	-H	<b>22</b>	no affinity
	-H	-H	-H	-H	<b>46</b>	no affinity
	-iPr	-iBu	-iPr	-H	<b>47</b>	450 ± 231
	-iBu	-H	-Ph	-H	<b>48</b>	no affinity
	-iBu	-H	-Ph	-Me	<b>49</b>	not soluble
	-iBu	-H	-(2-naphthyl)	-H	<b>50</b>	82.1 ± 11.0
	-iBu	-H	-(2-naphthyl)	-Me	<b>51</b>	not soluble

affinity 4-fold less than its 2-isopropoxy analogue **10**, suggesting the intramolecular hydrogen bond in **10** helps to orient the side chain and in turn to enhance binding. The importance of hydrophobic side chains was further confirmed by the weak binding of **36**, which lacks the key substituents. The series of terephthalamide derivatives with asymmetric substituents on the lower carboxamide group did not show activity in disrupting the Bcl-x<sub>L</sub>/Bak interaction (**22**, **46**–**49**, **51**) with an exception of **50**, possibly due to a different binding mode. These assay results confirmed that the terephthalamide derivatives retained the high in vitro affinity of the original terphenyl scaffold while reducing its complexity.

**(<sup>15</sup>N,<sup>1</sup>H)-2D-Amide Chemical Shift Perturbation Experiments.** The displacement of Bak peptide by terephthalamide in the fluorescence polarization suggests that the inhibitor and the peptide bind to the same surface area of Bcl-x<sub>L</sub> protein. To probe the binding mode of the terephthalamide, (<sup>15</sup>N,<sup>1</sup>H)-2D-amide chemical shift perturbation mapping with <sup>15</sup>N-labeled Bcl-x<sub>L</sub> was performed. Addition of **26** led to shifts in a number of residues on the surface of Bcl-x<sub>L</sub>. The residues of A89, G94, Y101, R102, L108, L112, A119, R139, and A142 showed significant chemical shift changes upon the addition of the synthetic inhibitor **26** (shown in magenta in Figure 4B). Some other residues, including E96, H113, I114, V127, I140, S145, and V161 (shown in yellow in Figure 4B), showed moderate

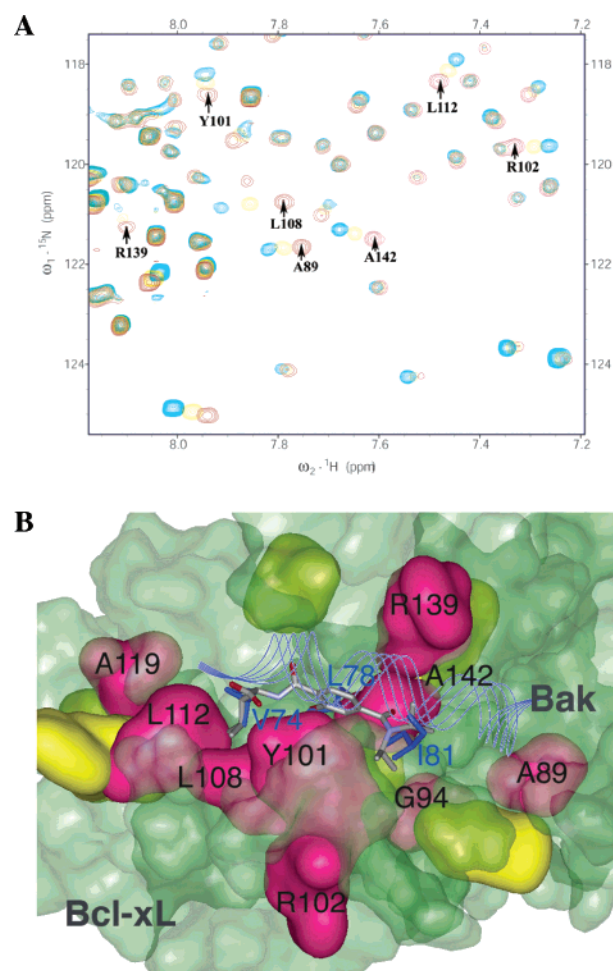


**Figure 4.** (A) <sup>15</sup>N HSQC spectrum recorded on <sup>15</sup>N-labeled Bcl-x<sub>L</sub> protein (2 × 10<sup>−3</sup> M solution in PBS) in the absence (blue) and in the presence of 0.5 equiv (cyan) and 1.0 equiv (red) of terephthalamide **26** added. Residues A89, G94, Y101, R102, L108, L112, A119, R139, and A142 show significant chemical shift change upon the addition of **26**. (B) Superimposition of top ranked result of the molecular-docking studies of **26** and Bak peptide. The residues that showed significant and moderate chemical shift change upon the addition of **26** are shown in magenta and yellow, respectively. The critical binding residues V74, L78, and I81 of the Bak peptide are shown in stick representation.

chemical shift change under the same conditions. These affected residues all lie in the shallow cleft on the protein into which the Bak helix binds. Overlay of **26** and the Bak peptide within the binding pocket suggests that the terephthalamide is indeed mimicking the cylindrical shape of the helix with the substituents making a series of hydrophobic contacts with the protein (Figure 4B). The residues V74, L78, and I81 of Bak BH3, which the terephthalamide has been designed to mimic, are within 4 Å of residues F97, R102, L108, I140, and A142 of Bcl-x<sub>L</sub>, all of which showed significant chemical shift changes upon addition of helical mimetic **26**. The effect on F97 was unclear due to overlap with N5 although it seems to shift significantly. These results confirmed that terephthalamide **26** targets the same cleft which the Bak BH3 peptide recognizes.

Comparison of these results with <sup>15</sup>N, <sup>1</sup>H-HSQC mapping of the previously reported terphenyl **1** (R<sub>1</sub> = R<sub>3</sub> = *i*Bu, R<sub>2</sub> = 1-naphthylmethylene) suggested a similar binding mode to Bcl-x<sub>L</sub> for both *proteomimetics*.<sup>11</sup> The residues most affected by both of the inhibitors are G94 in BH3, R102 and 108 in the C-terminal region of BH2, and R139, I140, and A142 in BH1

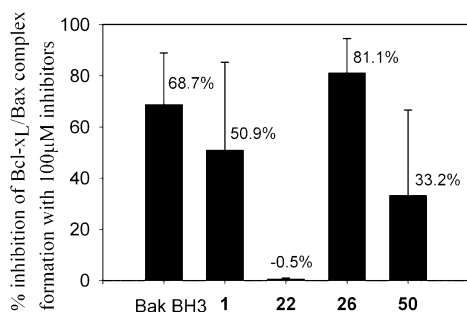


**Figure 5.** Results of the double transfection cellular assay (each percentage value is an average of three independent experiments).

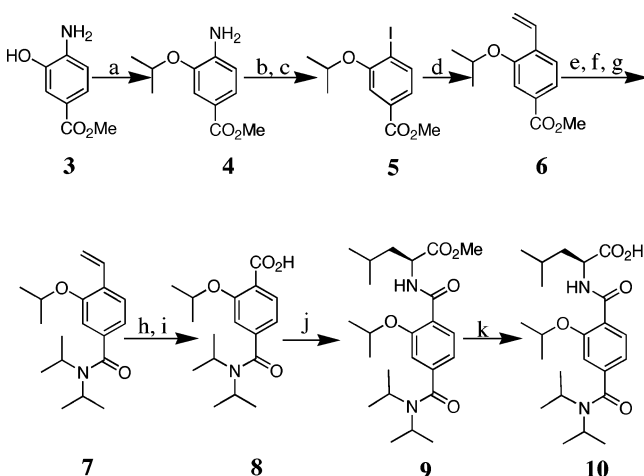
domain of Bcl-x<sub>L</sub>. These residues are all found in the conserved hydrophobic pocket on Bcl-x<sub>L</sub> where the Bak BH3 helix binds.<sup>14</sup> The chemical shift perturbation of these or their neighboring residues listed above indicated that both inhibitors and the Bak BH3 peptide target the same area on the Bcl-x<sub>L</sub> exterior surface, suggesting that terephthalamide is a successful alternative scaffold to terphenyl as a mimetic of  $\alpha$ -helices.

**Computational Docking Studies.** A computational docking study using the Autodock 3.0 program lent further support to the proposal that the binding cleft for the BH3 domain of the Bak peptide on the surface of Bcl-x<sub>L</sub> is the target area for the synthetic inhibitors. Over 90% of the conformational search results showed the terephthalamide docked to this region. Figure 4B shows the overlay of the top-ranked docking result, which was predicted to have a favored  $-10.28$  kcal/mol mean docked energy, with the BH3 domain of the Bak peptide in the Bcl-x<sub>L</sub>/Bak complex, suggesting that the side chains of the terephthalamide scaffold have an analogous spatial arrangement to the three key alkyl side chains of the Bak BH3 peptide.

**Inhibition of Bcl-x<sub>L</sub>/Bax Association in Intact Human Cells.** Human HEK293 cells were used to determine if terephthalamide derivatives inhibit the Bcl-x<sub>L</sub>/BH3 domain interaction in a cellular environment. HEK293 cells transfected with both HA-Bcl-x<sub>L</sub> and flag-Bax, an analogue to Bak, were treated with terephthalamide derivatives. After 24 h incubation, the cells were harvested and lysed. HA-tagged Bcl-x<sub>L</sub> protein was collected via immunoprecipitation with HA antibody. The resulting immunoprecipitates were loaded on to a 12.5% SDS-PAGE gel, and proteins transferred to nitrocellulose for western blots analysis. The presence of Bax protein was probed with anti-flag antibody. The inhibitory potencies of the terephthalamide compounds were determined by measuring the relative intensity of Bax protein bound to Bcl-x<sub>L</sub>. Treatment of HEK293 cells with terephthalamide **26** (100  $\mu$ M) resulted in inhibition of the association of Bcl-x<sub>L</sub> with Bax with an average value of  $81.1 \pm 13.5\%$  (Figure 5). Treatment of HEK293 cells with various concentrations of **26** resulted in an IC<sub>50</sub> of 35  $\mu$ M. Terphenyl **1** (R<sub>1</sub> = R<sub>3</sub> = *i*Bu, R<sub>2</sub> = 1-naphthylmethylene) inhibited the Bcl-x<sub>L</sub>/Bax association by only  $50.9 \pm 34.5\%$  at a concentration of 100  $\mu$ M. This result suggests that terephthalamide **26** is able to perturb Bcl-x<sub>L</sub>/Bax interaction in a cellular environment and that it has good membrane uptake properties.

In conclusion, a novel family of Bcl-x<sub>L</sub> antagonists, based on a terephthalamide mimic of  $\alpha$ -helical presentation of side chains, has been developed. A library of terephthalamide derivatives was prepared in a modular fashion and good in vitro affinities were observed using fluorescence polarization binding assays. The binding mode of a potent terephthalamide was

**Scheme 1.** Modular Synthesis of Terephthalamide Derivatives **9** and **10**<sup>a</sup>



<sup>a</sup> Reagents and conditions: (a) 2-iodopropane, K<sub>2</sub>CO<sub>3</sub>, acetone, reflux; (b) NaNO<sub>2</sub>, H<sub>2</sub>SO<sub>4</sub>, MeOH, H<sub>2</sub>O, 0 °C; (c) KI, Cu (bronze), reflux; (d) tributyl(vinyl)tin, Pd(PPh<sub>3</sub>)<sub>4</sub>, toluene, reflux; (e) NaOH(aq), MeOH; (f) (COCl)<sub>2</sub>, DMF, CH<sub>2</sub>Cl<sub>2</sub>; (g) (*i*Pr)<sub>2</sub>NH, CH<sub>2</sub>Cl<sub>2</sub>; (h) OsO<sub>4</sub>, NaIO<sub>4</sub>, tBuOH: CCl<sub>4</sub>:H<sub>2</sub>O (2:1:1); (i) pyridinium dichromate, DMF; (j) L-leucine methyl ester hydrochloride, 1-hydroxybenzotriazole hydrate, 1-[3-(dimethylamino)propyl]-3-ethylcarbodiimide hydrochloride; (k) KOH, MeOH.

confirmed by computational simulations and NMR spectroscopy. Experiments using intact human cells showed that the terephthalamides are able to disrupt the Bcl-x<sub>L</sub>/Bax BH3 domain interaction in cell-based assays.

## Experimental Section

**Inhibitor Preparation.** A modular synthesis of terephthalamide derivative **10** is shown in Scheme 1. The 2-isopropoxy group was introduced by O-alkylation. Sandmeyer reaction was used to introduce the iodo-substituent in **5**. A vinyl group was installed through Stille coupling, followed by hydrolysis of the methyl ester to generate a carboxylic acid at the 4-position. The lower amide bond formation was accomplished using diisopropylamine to attack the corresponding acid chloride intermediate to afford **7**. The 1-vinyl group was converted to a carboxylic acid by Lemieux–Johnson and Corey–Schmidt oxidation. Terephthalamide **9** was obtained by using standard peptide coupling of **8** and L-leucine.

**Fluorescence Polarization Assays.** Fluorescence polarization experiments were conducted on a Photon Technology International instrument using a 0.3 cm path length cuvette. Spectra were measured at 25 °C using 10.0 nm slit widths. Fluorescein-labeled Bak peptide (FI-GQVGRQLAIGDDINR-CONH<sub>2</sub>) was purchased from the HHMI Biopolymer/Keck Foundation Biotechnology Resource Center at the Yale University School of Medicine (New Haven, CT). The N-terminus of the peptide was capped with the fluorophore and the C-terminus was amidated. Bcl-x<sub>L</sub> was expressed and purified as previously described.<sup>7</sup> Excitation at 495 nm was used for the fluorescein-containing peptide and the excimer emission maximum at 535 nm was monitored. Polarization measurements were recorded upon titration of inhibitors (ca. 10 mM stock solutions in DMSO) at varying concentrations into a solution of 15 nM FI-Bak and 184 nM Bcl-x<sub>L</sub> (25 °C, 10.0 mM PBS, pH 7.4). Regression analysis was carried out using SigmaPlot 2001 (Systat Co.) ligand binding macro module. Experimental data were fitted into eq 1 to determine the IC<sub>50</sub> values, which in turn can be related to the known affinity of the 16-mer Bak peptide ( $K_d = 120$  nM) to acquire the inhibitory constant  $K_i$ .<sup>11,20</sup>

$$y = \min + (\max - \min) / (1 + 10^{x - \log \text{IC}_{50}}) \quad (1)$$

( $y$  = total binding,  $x$  = log concentration of ligand, min = nonspecific binding, max = maximum binding in absence of ligand)

**(<sup>15</sup>N,<sup>1</sup>H)-Amide Chemical Shift Perturbation Experiments.** (<sup>15</sup>N,<sup>1</sup>H)-2D-HSQC spectra were recorded on a Varian DPX-600 spectrometer. The concentration of Bcl-x<sub>L</sub> was 2.0 mM, with 0, 1.0 mM, and 2.0 mM **26**, respectively, in 10% DMSO/D<sub>2</sub>O (25 °C, 10.0 mM PBS, pH 7.0).

**Docking Studies.** The docking studies were performed using AutoDock 3.0.<sup>21</sup> A genetic algorithm (Lamarckian genetic algorithm, or LGA for short) was used and the torsion angles of the ligand were varied using AUTOTORS. All other procedures for the docking experiment were followed as described in the users manual for the AUTODOCK program. Docked conformations were ranked automatically by the AUTODOCK program using a force field scoring function. A total of 100 distinct conformational clusters were found out of 100 runs using an rmsd tolerance of 1.0 Å. Among those, one of the highest ranked docked structures was used for molecular visualization.

**Disruption of Bcl-x<sub>L</sub>/Bax Association in Whole Cells.** The anti-flag antibody (M2 mouse monoclonal) was purchased from Sigma-Aldrich. HEK293 cells were plated at an appropriate density 24 h prior to transfection and incubated overnight. Mirus LT-1 transfection reagent

(6 μL) was added dropwise into 100 μL of serum free RPMI medium and incubated at room temperature for 20 min. A total of 2 μg of pcDNA<sub>3</sub> HA-Bcl-x<sub>L</sub> and 2 μg of pCMV<sub>2</sub> Flag-Bax were added to the diluted transfection reagent and mixed by gentle pipetting. The transfection reagent/DNA complex was added dropwise to the cells and the cells were gently rocked. The cells were then incubated for 24 h with media solution containing various concentrations of terephthalamide compounds. The cells were scraped in PBS and lysed in NP-40 lysis buffer. HA-tagged Bcl-x<sub>L</sub> protein was collected via immunoprecipitation with HA antibody, washed and resuspended in Laemmli buffer (2×). The resulting mixture was loaded on to a 12.5% SDS-PAGE gel for protein separation, then transferred to nitrocellulose for western blots analysis. The presence of Bax was probed with anti-flag antibody. The inhibitory potency of the terephthalamide compounds was determined by measuring the relative intensity of Bax protein bound to Bcl-x<sub>L</sub>.

**Acknowledgment.** We thank the National Institutes of Health for financial support of this work.

**Supporting Information Available:** Scheme S1–S3, general synthesis procedures, compound characterization. This material is available free of charge via the Internet at <http://pubs.acs.org>.

JA0446404

- (21) Morris, G. M.; Goodsell, D. S.; Huey, R.; Olson, A. J. *J. Comput.-Aided Mol. Des.* **1996**, *10*, 293–304. Morris, G. M.; Goodsell, D. S.; Halliday, R. S.; Huey, R.; Hart, W. E.; Belew, R. K.; Olson, A. J. *J. Comput. Chem.* **1998**, *19*, 1639–1662. Goodsell, D. S.; Olson, A. J. *Proteins: Struct., Funct. Genet.* **1990**, *8*, 195–202.